Experimental Research on the Absorption of Fluorine in gamma-TiAl during Electroslag Remelting

P. Spiess[1], B. Friedrich[1]
[1]IME Process Metallurgy and Metal Recycling, RWTH Aachen University, D-52056 Aachen, Germany

Keywords: TiAl, Recycling, PESR, Halogen Effect, Fluorine

Abstract

In literature, it has been reported that the so called "halogen effect" significantly improves the oxidation resistance of gamma-TiAl. This effect is based on the formation of gaseous Al-halides which are oxidized to Al_2O_3 on the surface resulting in a protective alumina layer. To investigate the absorption of fluorine in gamma-TiAl during electroslag remelting and to enhance the oxidation resistance of the produced alloy by bulk-fluoridation, a series of tests was performed at IME. In a 400 kW lab scale furnace multiple electrodes of Ti-45Al were remelted using an active Ca-CaF_2 slag. Parameters like melt rate and Ca content in the slag were systematically varied. The ingots were sectioned and characterized by GDOS and EPMA to demonstrate the influence of the melting parameters on the efficiency of fluoridation as well as their impact on solidification structure with special regard to the distribution of fluorine.

Introduction

The development of structural intermetallic alloys for industrial use has been a focus since the 1980s. Especially the group of titanium aluminides is characterized by its very good properties like high melting point (about 1450 °C), low density (3.9 – 4.1 g/cm³) high specific elasticity modulus, good oxidation resistance up to 700 – 800 °C and high specific creep resistance (39 – 46 GPa cm³ g^{-1}). Due to the steady increasing use of titanium in airframes (cf. Figure 1) and TiAl in combustion engines as an alternative to superalloys, fuel consumption as well as pollutant emissions can be reduced significantly. [1-3] Because of confidentiality no precise information on the TiAl content in combustion engines are available.

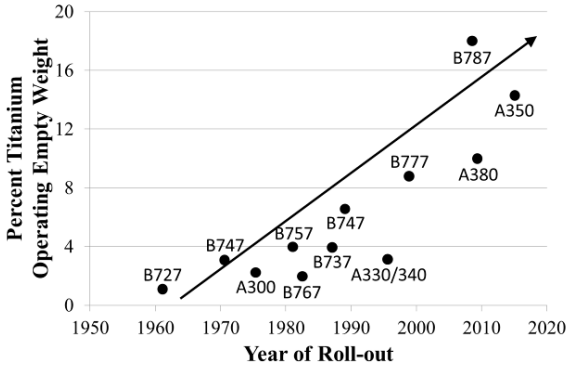

Figure 1: Titanium usage on Boeing Aircraft [4]

To further increase the efficiency of combustion engines it is appropriate to raise their operating temperature. However, operating temperatures above 800 °C lead to a considerable drop of the oxidation resistance of TiAl, due to the formation of an oxide layer consisting of Al_2O_3 and TiO_2. Both oxides have different rates of growth and expansion coefficients resulting in crack formation in the oxide layer. Although the oxidation protection can be increased by the addition of niobium since niobium lowers the Al activity. Niobium is attached to the Ti sub-lattice of α_2-Ti_3Al and γ-TiAl structure and influences the kinetics of flaking, whereby a finer grain structure is achieved. However, niobium contents above 2 wt.-% lead to a massive drop of Al activity which prevents the formation of Al_2O_3. Given that TiO_2 is a weak oxygen barrier the oxygen diffusion is accelerated. [5-6] Schütze [6] observed that the oxidation resistance can be further increased by microalloying of halogens like chlorine, iodine, bromine or fluorine, whereas Donchev [7] identified that only fluorine leads to a sustained increase of the oxidation resistance. This is based on the so called "halogen effect", wherein small amounts of a halogen are added into the alloy surface. At high temperatures the deposited fluorine in the metal edge zone selectively forms Al-fluorides, which shift through pores and microcracks to the metal surface. Due to the increasing oxygen partial pressure the fluorides decay and form gaseous F_2 and a dense Al_2O_3 layer.

The TiAl recycling process developed at IME consists of multiple industry approved processes and is explicitly explained by Reitz [8]. It is based on the deoxidization of via vacuum induction melting (VIM) consolidated casting scrap by pressure electroslag re-melting (PESR). To achieve a designated refining and deoxidization of the metal during PESR a reactive slag consisting of CaF_2 and metallic Ca is used. Due to its low vapour pressure, physical properties and good availability Nafziger [9] identified CaF_2 as the most suitable flux for ESR of titanium and titanium alloys. Because of the thermodynamic effects during ESR of titanium at high temperatures of around 1800 °C, CaF_2 decomposes (cf. eq. 1). By reaction of existant atomic fluorine radicals with the liquid metal, titanium fluorine TiF is formed (cf. eq. 2) and dissolves in the melt (cf. eq. 3).

$$(CaF_2) = \{CaF\} + \{F\} \quad \text{with } \Delta G_{R,1} \tag{1}$$

$$(Ti) + \{F\} = \{TiF\} \quad \text{with } \Delta G_{R,2} \tag{2}$$

$$\{TiF\} = [TiF]_{Ti} \quad \text{with } \Delta G_{R,3} \tag{3}$$

Scholz [10] reported that fluorine contents of 60 ppm after ESR of titanium are unavoidable. To obtain a positive effect of the F-effect on the oxidation resistance, an expected fluorine content of up to 500 ppm is needed. Since there is almost no thermodynamic data for equilibrium calculations between TiAl and CaF_2 as well as for evaporation tendencies, the conducted investigations engage on the experimental research on the absorption of fluorine in TiAl.

Experimental

In order to investigate the influence of the used process parameters on the fluorine absorption multiple remelting trials with a specific variation of single parameters were performed. The experiments were conducted at IME Process Metallurgy and Metal Recycling, Department and Chair of RWTH Aachen University.

Electroslag Re-melting Furnace (ESR)

Based on the method of electro-slag welding (ESW) in the 1880s Slavyanov developed the electroslag re-melting process. [11] An overview of the basic operating mode of ESR gives the subsequent Figure 2.

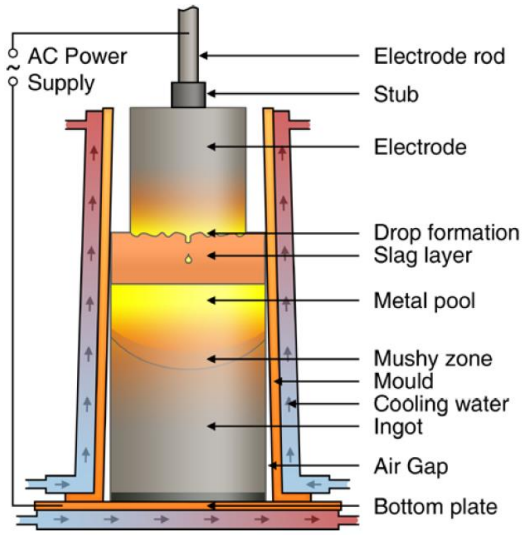

Figure 2: Principle design of an ESR furnace [12]

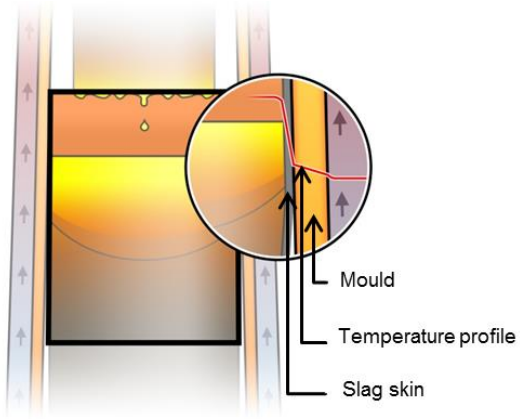

Figure 3: Heat removal during the ESR process [12]

During the electroslag re-melting process a self-consumable electrode is gradually molten by contact with a defined liquid slag. The dripping metal sinks through the slag while solid inclusions with a melting temperature higher than that of the base-metal will float into the slag. However, this float will only take place if the solid inclusions possess a lower density than the molten base-metal. Depending on the chemical properties and density of the inclusions they can be dissolved in the slag. The dripping metal solidifies partly directional in a water cooled copper crucible. [13]

Experimental Setup

The IME pressure electroslag remelting furnace used for the investigations (cf. Figure 4) is controlled by means of computer-aided software. As feedstock electrodes with a maximum length of 1340 mm and a diameter of up to 110 mm can be used. The available water-cooled molds have a height of up to 900 mm and an inner diameter of about 170 mm. The closed system can be at pressures up to 50 bar. The power supply of the furnace is carried out by a thyristor control, where an operating voltage of 80 V and a current of 5 kA, 66.6 V and 6 kA respectively can be tapped. Both cases result in a maximum power output of approximately 400 kW.

Figure 4: IME **P**ressure **E**lectro**S**lag **R**emelting furnace (PESR)

The experiments were performed in the PESR in closed state. An 890 mm high conical copper mold with a removable bottom plate was used. Its lower diameter is 170 mm while its upper diameter is 154 mm. A starting plate made of TiAl sputter targets (cf. Figure 5) is placed on the crucible bottom to ensure electrical contact during the starting phase of the process. Then the crucible is filled with slag.

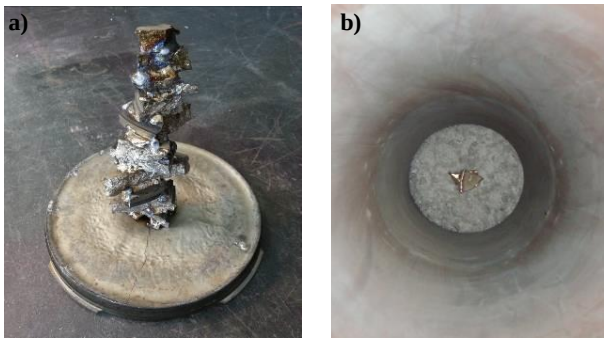

Figure 5: a) Starter box made of Ti-50Al sputter targets
b) Starter box in crucible surrounded by slag

As slag the technically pure CaF_2 slag Wacker Electroflux 2052 (> 97 wt.-% CaF_2) was used. According to the process requirements metallic calcium as deoxidization agent was added. For remelting, pressed Ti-45Al electrodes (cf. Figure 6) made of titanium sponge and aluminum rods with a length of 1200 mm and a circumference of 301 mm were used. The furnace pressure was chosen to 20 bar Ar. For this purpose and in order to avoid reactions with oxygen the vessel is evacuated to 1^{-10} mbar and bachfilled with Ar gas up to the desired pressure.

Figure 6: Pressed Ti-45Al electrode made from titanium sponge and aluminum rods

Experimental Procedure

After the setup of the furnace is completed, the process starts with an initial phase, whose process parameters are exemplified in the following Table I. Thereby the control of the process at the beginning is done by controlling the current and the voltage. After the first 3 steps the regulation is changed to power and resistance.

Table I: Exemplary presentation of the stepwise change of process parameters during initial phase of each PESR experiment

Step	Current	Voltage	Power	Resistance	Dwell
	/kA	/V	/kW	/mOhm	/min
1	3.0	38.0	60.0	8.0	0.2
2	5.5	40.0	60.0	8.0	3.0
3	5.0	40.0	100.0	8.0	3.0
4	4.0	40.0	100.0	8.0	2.0
5	4.0	40.0	145.0	9.0	2.0

After reaching the melting phase a selective variation of the process parameters was carried out to examine their influence on the fluorine content of the TiAl alloy used. The varied process parameters are the remelting power as well as the amount of added deoxidization agent. An overview of the five PESR trials carried out with identical electrodes and the process parameter settings used are given in the following Table II.

Table II: Selective variation of the process parameters during remelting phase

Trial	Power	Ca content in slag	Resistance
	/kW	/wt.-%	/mOhm
A	125.0	0.0	9.2
B	100.0	0.0	9.2
C	125.0	2.5	9.2
D	125.0	5.0	9.2
E	145.0	2.5	9.2

Trial A serves as a reference experiment in which an average power of 125 kW and 4.5 kg Electroflux 2052 slag without any addition of deoxidization agent were used. For investigation of the influence of the remelting power in trial B the power has been reduced to 100 kW. Trials C and D are used to study the influence of the addition of deoxidization agent, where 2.5 wt.-% and 5.0 wt.-% respectively of the slag were replaced by calcium. Finally, in trial E the effect of an increased remelting power at medium calcium content in the slag was investigated.

After remelting the obtained ingots were sectioned and sampled in the mechanical workshop at IME and characterized by GDOS and EPMA. The detection limit for fluorine was 100 ppm.

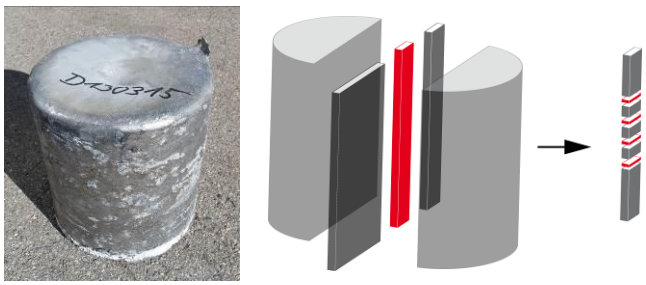

Figure 7: Sampling of the remelted material

Results

The prepared samples were analyzed both on the titanium and the aluminum content. The results are shown in the following Figure 8 and are compared with the composition of the used electrodes. In all experiments performed, a deviation between the targeted and the analyzed composition can be observed, whereas the deviation is illustrated by a raise of the aluminum content and a drop of the titanium content. The largest deviation with a value of 1.92 at.-% appears in Trial A, which was operated with a power of 125 kW (cf. Table II). Whereas in Trial B, the used remelting power of 100 kW results in a deviation of 1.19 at.-%. In both trials no calcium was added to the slag.

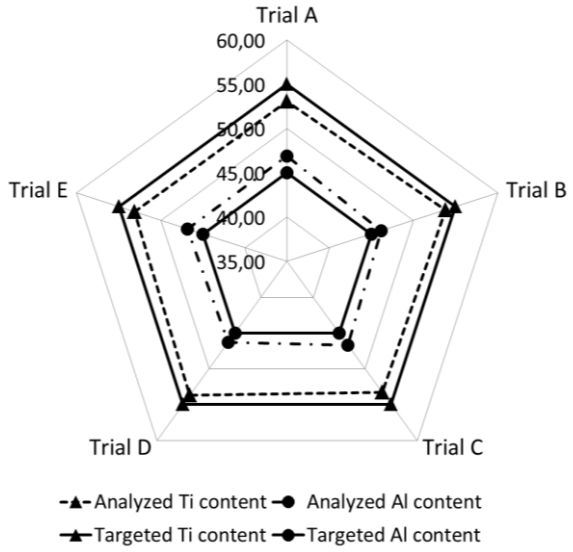

Figure 8: Analyzed and targeted aluminum and titanium content in remelted material

This effect is due to the nature of the used electrodes. As described in the experimental setup, the electrodes consist of pressed titanium sponge and aluminum rods. By reason of the lower melting temperature of aluminum compared to titanium, the aluminum rods melt down faster (cf. Figure 9) resulting in a slight raise of the aluminum content in the remelted ingot. This effect turns out the more, the higher the used remelting power.

Figure 9: Electrode tip after remelting with calcium addition

A similar effect can be observed in Trials C (1.69 at.-%), D (1.29 at.-%) and E (1.86 at.-%), where calcium was added to the slag. Due to the evaporation of calcium a thin vapor film is formed at the electrode tip and the appearance of arcs is advantaged. By the additional energy introduced more titanium is melted so that the deviation of the composition is lower than in melts without calcium addition. It can be observed that even a small addition of calcium to the slag results in a reduction of the deviation.

The following Figures 10 to 16 show the beam mapping of the prepared samples via electron beam back-scatter detector as well as the distribution of oxygen, fluorine, titanium and aluminum in the samples. The metallographic examination reveals only small differences in the solidification structure.

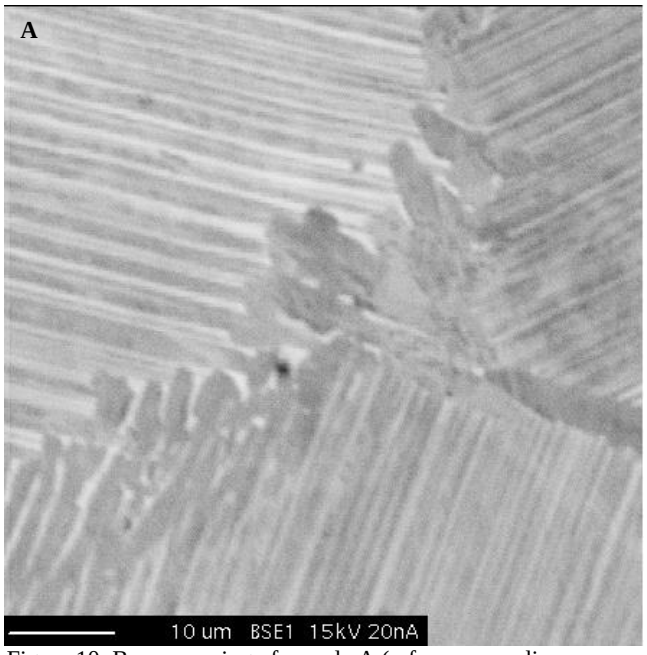

Figure 10: Beammapping of sample A (reference, medium power, no Ca addition) via electron beam back-scatter detector

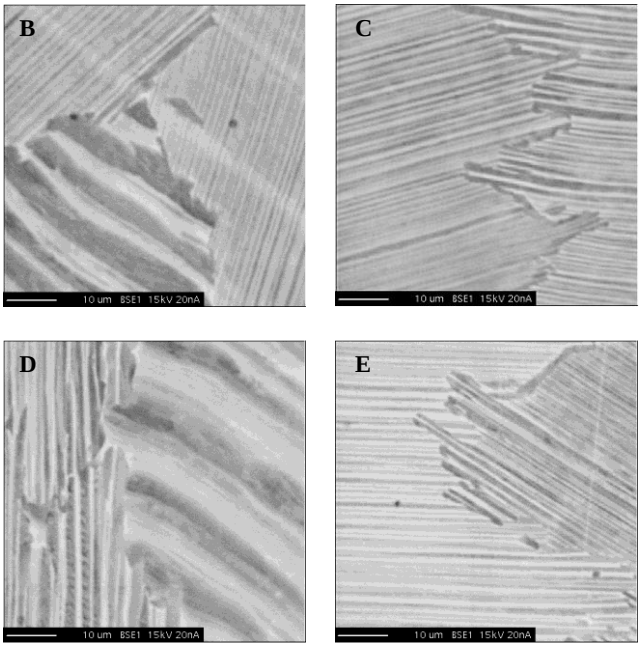

Figure 13: Beammapping of samples B, C, D and E via electron beam back-scatter detector

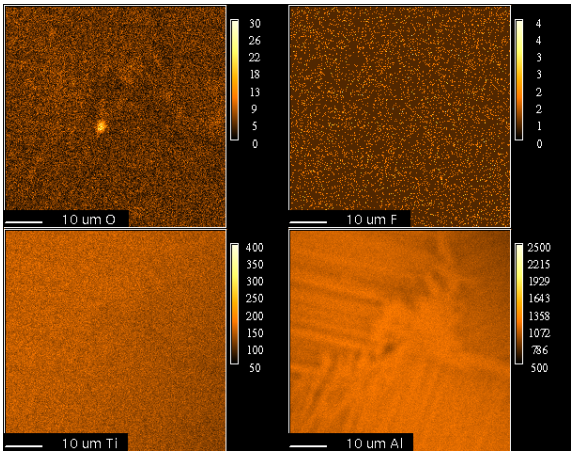

Figure 11: Distribution of O, F, Ti and Al in sample A (reference, medium power, no Ca addition); analyzed by EPMA

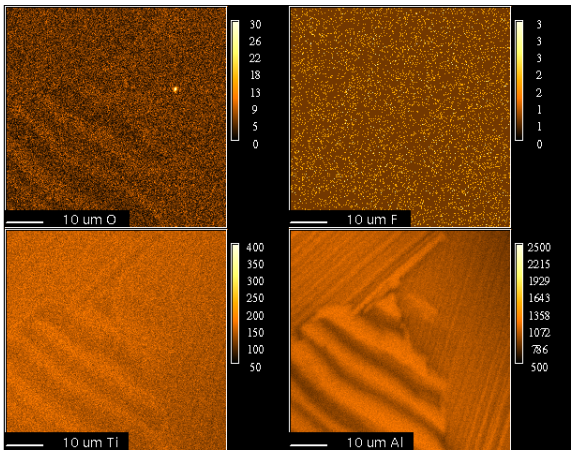

Figure 14: Distribution of O, F, Ti and Al in sample B (low power, no Ca addition); analyzed by EPMA

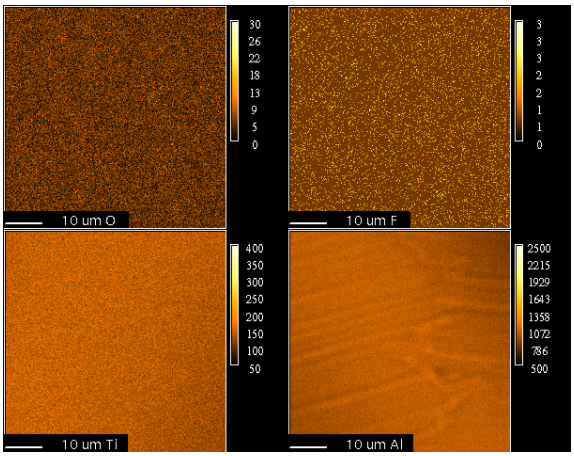

Figure 12: Distribution of O, F, Ti and Al in sample C (medium power, low Ca addition); analyzed by EPMA

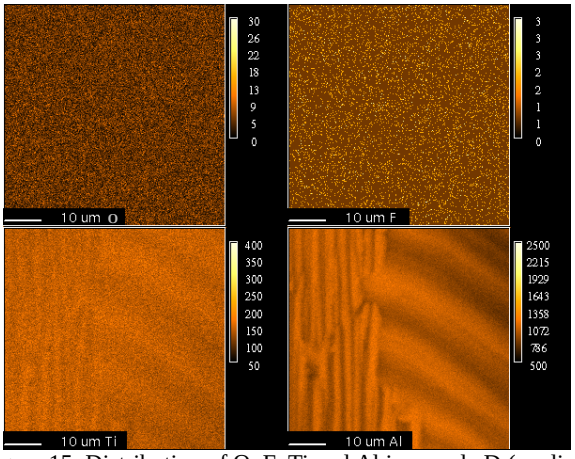

Figure 15: Distribution of O, F, Ti and Al in sample D (medium power, high Ca addition); analyzed by EPMA

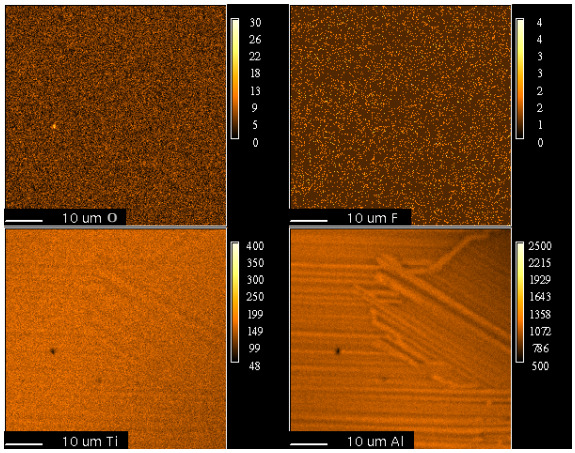

Figure 16: Distribution of O, F, Ti and Al in sample E (high power, low Ca addition); analyzed by EPMA

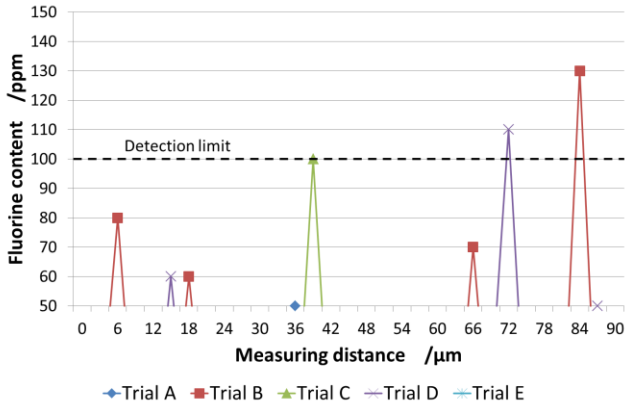

Figure 17: Results of the performed line scans for determination of fluorine

Upon closer examination of the oxygen distribution it can be seen that small nonmetallic inclusions (NMI) sporadically accumulate at the grain boundaries. These NMIs have a size of approximately 0.5 to 1 µm and occur primarily in the experiments without calcium addition (cf. Figure 11 and Figure 14). The background of adding calcium consists of the deoxidization of the used feedstock during remelting. In this case, by the reaction of the calcium dissolved in the slag with oxygen dissolved in the metal phase the development of calcium oxide is benefited. Furthermore, a reaction between the dissolved calcium and the nonmetallic inclusions takes places in which most of the NMIs get disbanded (cf. Figure 12 and Figure 15) or at least their size is reduced (cf. Figure 16). A complete removal of the nonmetallic inclusions is unlikely to be achieved.

A further effect of the calcium addition is the already mentioned decrease of the oxygen content. At detailed consideration of Figure 13-B and Figure 14, different oxygen contents between the titanium rich phase and the aluminum rich phase can be observed. Due to the large oxygen solubility in titanium, the oxygen content in the titanium rich phase is slightly higher than in the rest of the alloy. By deoxidization with metallic calcium the oxygen content is decreased what results in similar oxygen contents in both the titanium rich phase and the aluminum rich phase.

The determination of fluorine was carried out using electron probe micro-analysis with a fluorine detection limit of 100 ppm. As shown in Figures 11, 12, 14, 15 and 16 no fluorine in the bulk material above the detection limit could be determined. Hence, additional line scans were performed, whose results are shown in Figure 17. At rare intervals fluorine could be detected, whereas only in sample B and sample D the detection limit was exceeded. Therefore, it can be assumed that in case of an active CaF_2 slag the investigated process parameters (power and Ca addition) have a subordinated influence on the fluorine adsorption in γ-TiAl during pressure electroslag remelting. Higher fluorine contents than the reported value by Scholz (60 ppm) [10] could not be achieved in this investigation.

Nevertheless, even no fluorine could be detected at the grain boundaries. This suggests that there is no or at least a negligible deposition of CaF_2 on the grain boundaries what could have a negative influence on the mechanical properties.

Conclusions

(1) The electron probe micro-analysis has shown that the used electrode design caused increased aluminum contents in the remelted material. This effect can be reduced by the addition of even small amounts of calcium to the slag.

(2) Small nonmetallic inclusions with a size of 0.5 to 1 µm can occasionally be observed which primarily accumulate at the phase boundaries. By the addition of calcium to the slag both the NMIs frequency of occurrence as well as their size can be reduced. A complete removal of the nonmetallic inclusions is unlikely to be achieved.

(3) The usage of a pure and an active CaF_2 slag respectively leads to no significant fluorine enrichment and thereby no positive effect on the halogen effect. However, there is no deposition of CaF_2 on the grain boundaries.

Outlook

Due to the thermal stability of CaF_2 a partial substitution of the slag is considered in further investigations. Particular attention will be paid on the two compounds MgF_2 and NaF_2. Furthermore, there will be an exchange of the analysis methodology. By use of glow discharge mass spectrometry (GDMS) detection limits in the ppb range become feasible.

References

1. E.A. Loria, “Quo vadis gamma titanium aluminide,” *Intermetallics*, 9 (2001), 997-1001
2. H. Clemens, “ Intermetallische Werkstoffe für Anwendungen in Automobil- und Flugzeugtriebwerken,” *BHM Berg- und Hüttenmännische Monatshefte*, 153 (2008), 337-341
3. S. Knippscheer, and G. Frommeyer, „Neu entwickelte TiAl-Basislegierungen für den Leichtbau von Triebwerks- und Motorenkomponenten – Eigenschaften, Herstellung, Anwendung,” *Materialwissenschaft und Werkstofftechnik*, 37 (2006), 724-730
4. S. Seagle et al., *Titanium – The Ultimate Choice* (Broomfield, CO: International Titanium Association, 2007)
5. P.J. Masset, “Influence of alloy compositions on the halogen effect in TiAl alloys,” *Materials and Corrosion*, 59 (2008)
6. M. Schütze, “The halogen effect in the oxidation of intermetallic titanium aluminides,” *Corrosion Science*, 44 (2002)

7. A. Donchev, “Improvement of the oxidation behavior of TiAl-alloys by treatment with halogens,” *Intermetallics*, 14 (2005), 1168-1174
8. J. Reitz, C. Lochbichler, and B. Friedrich, „Recycling of gamma titanium aluminide scrap from investment casting operations“, Intermetallics, 19 (2011), 762-768
9. R.H. Nafziger, “Slag compositions for Titanium Electroslag Remelting and Effects of Selected Malting Parameters”, *Proceedings of Second International Symposium on Electroslag Remelting Technology*, (1969)
10. H. Scholz et al., “An Advanced ESR Process for the Production of Ti-Slabs”, *Ti-2003 Science and Technology*, ed. G. Lütjering and J. Albrecht (Weinheim, Wiley-VCH-Verlag, 2004), 205-212
11. B.I. Medovar, “Electroslag remelting of alloy steel,” *Metallurg*, 4 (1970), 32-35
12. N. Giesselmann et al., “Numerical simulation of the electroslag remelting process in order to determine influencing parameters on ingot defects,” *Proceedings of the 1st International Conference on Ingot Casting, Rolling and Forging*, (2012)
13. B. Friedrich, C. Lochbichler, and J. Reitz, „Closing The Material Cycle of Titanium – Thermochamical and Experimental Validation of a New Cycling Concept,“ *Proceedings of the 2007 International Symposium on Liquid Metal Processing and Casting*, (2007)